POLITECNICO DI TORINO
Repository ISTITUZIONALE

Swept Notch NPR for Linearity Assessment of Systems Presenting Long-Term Memory Effects

(Article begins on next page)

26 September 2024

Swept Notch NPR for Linearity Assessment of Systems Presenting Long-Term Memory Effects

Ricardo Figueiredo*†, Anna Piacibello‡, Vittorio Camarchia‡,Nuno Borges Carvalho*†

*Universidade de Aveiro, Portugal, †Instituto de Telecomunicações, Portugal, ‡Politecnico di Torino, Italy.

Abstract—**Mobile and Satellite applications are progressively moving towards broader bandwidths, so nonlinear long-term memory effects manifested by RF Transmitters must not be neglected. This trend evidences the need for more informative and robust broadband linearity metrics.**

This work proposes swept notch noise power ratio to capture co-channel long-term memory effects, moving the scientific discussion toward the definition of useful metrics for broadband nonlinear memory assessment.

Index Terms—**intermodulation distortion, long-term memory effects, nonlinear, noise power ratio.**

I. Introduction

Broadband transmitters suffer from long-term memory effects that cannot be neglected. Moreover, existing linearity metrics lack robustness to guide standardization, design and to define safe operation regimes in terms of long-term memory.

Noise power ratio (NPR) is the traditional benchmark for Satellite PA linearity assessment [1], [2]. NPR characterization consists in exciting a device with a band-limited addictive white Gaussian noise (AWGN) signal with a central notch, as shown in Fig. 1, and evaluate the ratio between the output power spectral density (oPSD) within the AWGN excitation and the oPSD within the notch [3]. NPR is thus given by

$$NPR = \frac{oPSD_{AWGN}}{oPSD_{Notch}}. \tag{1}$$

In other words, NPR averages the intermodulation distortion (IMD) within the notch for a given signal oPSD. Note that this NPR definition is a narrow-band approximation, since it assumes that evaluating the IMD within the central notch provides the best approximation for the average IMD along the signal bandwidth.

Several works have studied how IMD manifests in-band [4]–[6], and it is well documented that for the memoryless case the uncorrelated IMD maximum occurs at the central excitation frequency. Thus, the use of a central notch when evaluating NPR is reasonable in a memoryless system since this tends to overestimate the average IMD. However, results shown in the aforementioned studies also indicate that in the presence of long-term memory effects the uncorrelated IMD maximum might no longer occur at the central excitation frequency. Thus, the use of NPR to assess the linearity of systems presenting long-term memory effects might be misleading, and must therefore be critically studied.

This work presents that study, tackling NPR linearity assessment limitations in the presence of long-term memory effects. First, we explain how different long-term memory effects can
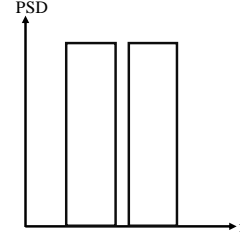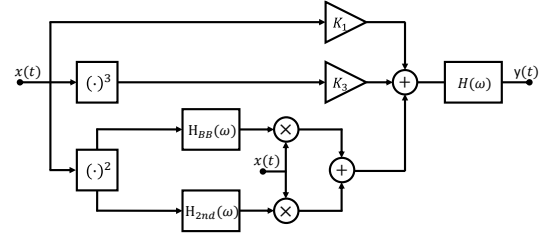

Fig. 1: Noise Power Ratio Excitation Signal.

Fig. 2: Broadband RF System Model Under Study.

produce different co-channel IMD profiles along the signal bandwidth and how NPR might misrepresent system linearity in such scenarios. Then, we propose the swept notch NPR characterization procedure, which is capable of capturing long-term memory effects along the signal bandwidth. The novel characterization procedure is corroborated with experimental results.

II. Impacts of Long-Term Memory Effects on NPR

To exemplify how long-term memory effects can impose different co-channel IMD profiles along the signal bandwidth, a demonstrative three-slice model, based on [7] and shown in Fig. 2, is used. It is composed by a dominant linear slice, a 3_{rd} order memoryless nonlinearity and a 3_{rd} order nonlinearity with memory imposed by upconverted baseband components and downconverted 2nd harmonic components. Since we want to analyze memory effects, let's consider an operation regime where the nonlinearity with memory is dominant over the memoryless nonlinearity, i.e. IMD is mostly imposed by the 3_{rd} slice. Let's also consider that the system is excited by a multi-sine with equally spaced tones.

In such scenario, after the squarer, $(\cdot)^2$, IMD components appear at frequencies
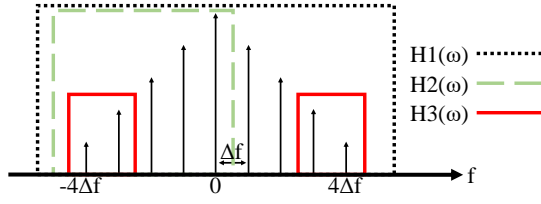
$$\omega_{2nd} = \omega_{q1} + \omega_{q2}, \tag{2}$$

Fig. 3: IMD products near DC and 2_{nd} harmonic for a 5 tone excitation and examples of possible H_{BB} and H_{2nd} filter profiles: $H_1(\omega)$; $H_2(\omega)$; $H_3(\omega)$.

TABLE I: Number of IMD products up/down converted to ω_n from frequencies spaced $n\Delta f$ from DC and 2_{nd} Harmonic.

$n\Delta f$	-4	-3	-2	-1	0	1	2	3	4
ω_1	1	2	3	4	5	0	0	0	0
ω_2	0	2	3	4	5	4	0	0	0
ω_3	0	0	3	4	5	4	3	0	0
ω_4	0	0	0	4	5	4	3	2	0
ω_5	0	0	0	0	5	4	3	2	1

where ω_{q1} and ω_{q2} can take the value of any tone frequency of the multi-sine excitation, either positive or negative. Thus, products where $sgn(\omega_{q1}) \neq sgn(\omega_{q2})$ constitute baseband IMD, while products where $sgn(\omega_{q1}) = sgn(\omega_{q2})$ constitute second harmonic IMD. Fig. 3 displays these IMD products around DC and the 2_{nd} harmonic for a 5 tone excitation.

After the $H_{BB}(\omega)$ and the $H_{2nd}(\omega)$ filters, signals are mixed with $x(t)$. This operation generates IMD at the following frequencies

$$\omega_{3rd} = \omega_{2nd} + \omega_{q3}, \tag{3}$$

where w_{q3} can take the value of any tone frequency of the multi-sine excitation, either positive or negative. Thus, some baseband IMD is up-converted to the co-channel, while some 2_{nd} harmonic IMD is down-converted. However, the number of IMD products converted to each excitation tone depends on the separation from either DC or the 2_{nd} harmonic of the IMD products shown in Fig. 3. This dependence is listed in Table I for a 5 tone excitation. As shown, more products overlap near the central frequency, ω_3, as expected in a memoryless system.

After laying this out, it is easy to understand how the memory introduced by filters $H_{BB}(\omega)$ and $H_{2nd}(\omega)$ can affect differently the co-channel IMD. If both filters have the profile of $H_1(\omega)$ in Fig. 3, co-channel IMD is not affected and presents a memoryless-like profile. However, if both filters have the profile of $H_3(\omega)$ in Fig. 3, only products spaced $\pm 3\Delta f$ and $\pm 4\Delta f$ from DC or the 2_{nd} harmonic are converted to the co-channel, meaning that no IMD products fall on ω_3, generating a central IMD minimum. On the other hand, if $H_{BB}(\omega)$ has the profile of $H_3(\omega)$ in Fig. 3 and $H_{2nd}(\omega)$ has the profile of $H_2(\omega)$ in Fig. 3, the number of IMD products monotonically decreases from ω_1 to ω_5. To illustrate these ideas a 101-tone excitation, replicating AWGN, with 1 MHz bandwidth at a carrier of 3 MHz is used to excite the system in Fig. 2. $H_{BB}(\omega)$ and $H_{2nd}(\omega)$ are designed using the principles
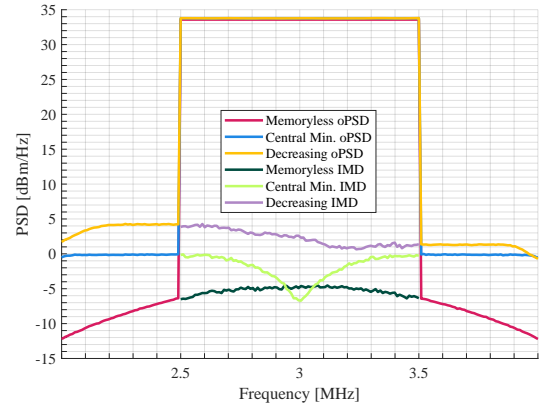

Fig. 4: Simulation results of the output PSDs and co-channel distortion PSD for each scenario described.
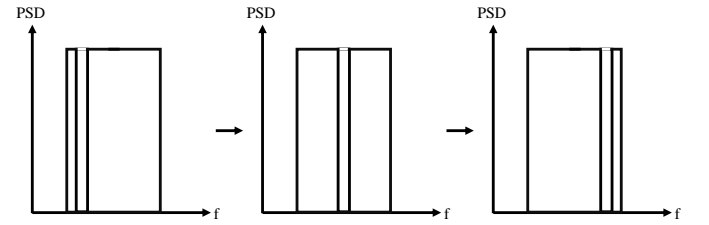

Fig. 5: Swept Notch NPR Excitation Concept.

previously described. Fig. 4 shows both the signal oPSD and the uncorrelated co-channel IMD obtained through simulation.

What is important to retain from this demonstrative analysis is that a classical NPR characterization procedure is unable to detect co-channel IMD variations due to long-term memory effects, like the decreasing IMD shown in Fig. 4; and that in some cases, like the central minimum co-channel IMD scenario portrayed in Fig. 4, a classical NPR characterization can critically underestimate IMD. Thus, better broadband linearity metrics are required.

III. SWEPT NOTCH NPR

A. Concept

The Swept Notch NPR concept consists in performing several NPR characterizations in which the notch is swept along the co-channel, as shown in Fig. 5, instead of performing a single measurement with a central notch.

The premise is that by doing this it is not only possible to determine the best co-channel frequency to evaluate the average co-channel IMD, as it is also possible to detect co-channel IMD variations due to long-term memory effects.

Fig. 6 presents the swept notch NPR simulation results for each scenario displayed in Fig. 4. Each "step" on the graph corresponds to a NPR measurement performed within the notch located in that co-channel frequency region. The notch used occupies 5% of the co-channel. As shown, swept notch NPR is capable of characterizing long-term memory effects along the co-channel, as it captures the inverted trend of IMD along the co-channel. Once again, this graph shows
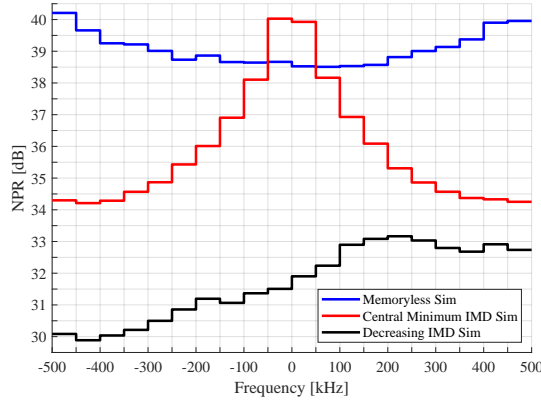
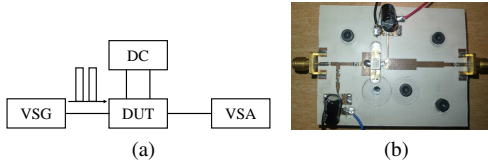Fig. 6: Simulated swept notch NPR of each described scenario.

Fig. 7: NPR Characterization: (a) Setup; (b) Device under test (DUT).

Fig. 8: Measured swept notch NPR of the ERA-2+ DUT at 5.67 GHz.

Fig. 9: Measured swept notch NPR of the GaN DUT at 2.6 GHz and 3.5 GHz.

the ineptitude of classical NPR characterization to evaluate IMD in caricature scenarios like the central minimum IMD, where it would underestimate the maximum IMD by 6 dB.

B. Experimental Validation

To validate the swept notch NPR proposal, this characterization procedure is tested experimentally. The setup, presented in Fig. 7a, consists in a R&S SMW200A VSG to generate the excitation signal and a R&S FSW VSA to measure the device under test (DUT) output signal. A 1001-tone excitation, replicating AWGN, with -10 dBm average power is used. The notch occupies 5% of the co-channel. Two DUTs are tested, the GaN PA shown in Fig. 7b biased near class B and an ERA-2+ PA from mini-circuits. The GaN PA is excited with a 100 MHz signal at both 2.6 GHz and 3.5 GHz, and the ERA-2+ is excited with a 50 MHz signal at 5.67GHz. Fig. 8 presents the swept notch NPR measurement of the ERA-2+, while Fig. 9 presents the measurements of the GaN PA.

The ERA-2+ results present a swept notch NPR centered around 18.4 dB and the NPR profile along the co-channel strongly indicates a memoryless behaviour, since NPR tends to improve toward the edges of the co-channel and to degrade toward the center, following a parabolic shape, as previously observed in the simulations shown in Fig. 6.

The GaN PA results present a swept notch NPR centered around 37.5 dB. The NPR profile along the co-channel at 3.5 GHz also tends to indicate a memoryless behaviour, but some asymmetry is observed between lower and upper frequencies in the co-channel, which might be due to long-term memory effects. On the other hand, the NPR profile along the co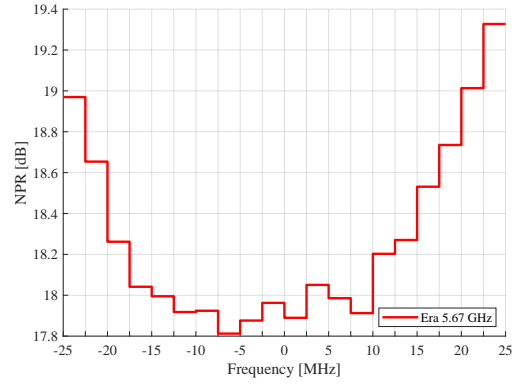-channel at 2.6 GHz clearly deviates from the memoryless behavior, oscillating between -30 MHz and 30 MHz. This indicates more strongly the manifestation of long-term memory effects. This profile is not like any of the simulated results shown in Fig. 6, meaning that the memory mechanisms of this DUT probably differ from those used for conceptualization.

Note that although we cannot guarantee the co-channel IMD variations observed are only due to long-term memory effects, these results validate the ability of swept notch NPR to capture co-channel IMD profiles that resemble and differ from the memoryless profile, and thus the ability of swept notch NPR to characterize co-channel IMD profile variations due to long-term memory effects.

IV. CONCLUSION

This work evidences the limitations of NPR to assess linearity in the presence of long-term memory effects.

To overcome such limitations, a swept notch NPR characterization procedure to detect the impacts of long-term memory effects on co-channel IMD was proposed and validated.

Further work is required to transform swept notch NPR in a quantifiable memory metric capable of extracting useful long-term memory effect models. But swept notch NPR is already

an initial step toward more robust and informative broadband linearity metrics.

REFERENCES

[1] G. Lasser, M. R. Duffy, and Z. Popović, "Dynamic dual-gate bias modulation for linearization of a high-efficiency multistage pa," *IEEE Transactions on Microwave Theory and Techniques*, 2019.

[2] S. Din, A. M. Morishita, N. Yamamoto, C. Brown, M. Wojtowicz, and M. Siddiqui, "High-power k-band gan pa mmics and module for npr and pae," in *2017 IEEE MTT-S International Microwave Symposium (IMS)*. IEEE, 2017, pp. 1838–1841.

[3] J. C. Pedro and N. B. Carvalho, *Intermodulation distortion in microwave and wireless circuits*. Artech House, 2003.

[4] J. P. Martins and N. B. Carvalho, "Co-channel and adjacent channel distortion in microwave amplifiers presenting memory," in *2007 European Microwave Conference*. IEEE, 2007, pp. 40–43.

[5] J. P. Martins, N. B. Carvalho, and J. C. Pedro, "Intermodulation distortion of third-order nonlinear systems with memory under multisine excitations," *IEEE transactions on microwave theory and techniques*, vol. 55, no. 6, pp. 1264–1271, 2007.

[6] S. Farsi, P. Draxler, H. Gheidi, B. K. Nauwelaers, P. Asbeck, and D. Schreurs, "Characterization of intermodulation and memory effects using offset multisine excitation," *IEEE Transactions on Microwave Theory and Techniques*, vol. 62, no. 3, pp. 645–657, 2014.

[7] A. Walker, M. Steer, K. Gard, and K. Gharaibeh, "Multi-slice behavioral model of rf systems and devices," in *2004 IEEE Radio and Wireless Conference*. IEEE, 2004, pp. 71–74.